Implementation of Active Training for an Upper-limb Rehabilitation Robot Based on Impedance Control

Liang Peng[1], Zeng-Guang Hou[1], Nikola Kasabov[2], Long Peng[1], Jin Hu[1], Weiqun Wang[1]

1. The State Key Laboratory of Management and Control for Complex Systems,
Institute of Automation, Chinese Academy of Sciences, Beijing, 100190
E-mail: {liang.peng, zengguang.hou, long.peng, jin.hu, weiqun.wang}@ia.ac.cn

2. Knowledge Engineering and Discovery Research Institute, Auckland University of Technology, Auckland
E-mail: nkasabov@aut.ac.nz

Abstract: Many rehabilitation robots have been designed to alleviate the conflict between increasing number of post-stroke patients and shortage of therapists. Active training is the main feature of advanced rehabilitation robots, which has been proved to be more effective than simple passive movement training. This paper presents the implementation of active training on a 2-DOF upper-limb rehabilitation robot, which can assist the shoulder and elbow joint rehabilitation training of post-stroke patients. The controller is built based on impedance control, which can provide a compliant human-robot reaction. The implementation of active training is combined with a virtual reality game, and the average error between the actual and target reaction force is 1.41 ± 0.79 N in the X axis, and 1.22 ± 0.91 N in the Y axis.

Key Words: Active Training, Rehabilitation Robot, Force Feedback, Impedance Control

1 INTRODUCTION

With the increasing number of stroke patients over the world, robot assisted rehabilitation has the potential to be a common therapy method for post-stroke rehabilitation. Robots are more appropriate to provide repetitive movement training than human therapists, and most conventional therapy programs are labor intensive and time-limited [1, 2].

During the last two decades, many rehabilitation robots have been designed and some of them have been commercialized and in clinical use, which helps release the burden of physical therapists. However, most advanced robots are still limited in labs or in rehabilitation institutes, since they are large in size, and complicated to set up [3]. As motor learning requires regular and intensive training, home-based rehabilitation is expected to be more efficient and economical for motor function recovery.

For this purpose, we have designed a novel upper-limb rehabilitation robot, which is compact in size and easy to set up, and active training can be realized attributed to its force feedback ability.

Active training is the main feature of most advanced rehabilitation robots, where the robot provides assistance or resistance according to the patient's motion intentions. As the motion is initiated and the interaction force is regulated according to the patient's voluntary efforts, active training is believed to be able to motivate the patient's participation and enhance their motor learning [4].

This research is supported in part by the National Natural Science Foundation of China (Grants 61225017, 61175076, 61203342), and the International S&T Cooperation Project of China (Grant 2011DFG13390).

However, active training poses a big challenge to the mechanical design and control of the robot. On one hand, the robot should be backdrivable, high-stiff and has low inertia. On the other hand, the interaction should be compliant and safe, which can not be achieved by the conventional motion control methods.

This paper focuses on the realization of force feedback and active training based on impedance control method. Impedance control is a commonly used method in compliant human-machine interaction, which allows the actual motion to deviate from the desired path, and the reaction force is regulated based on the motion errors according to some desired mechanical impedance characteristics.

The remaining parts of this paper are organized as follows. In section 2, basic design features of the robot are given, including the mechanical structure and control system architecture. In section 3, kinematic analysis of the robot are performed, which is the basis of robot control. In section 4, the realization of active training is presented in detail and the performance of the control method is given.

2 FEATURES OF THE ROBOT

2.1 Mechanical Structure

The mechanical structure of the robot is shown in Fig 1.

As shown in Fig 1, the robot is based on a five-bar parallel structure, which has two distal links and two proximal links, and a handle is installed at the end of the distal links. Two base joints are actuated while other joints are passive, which means the robot has two degrees of freedom (DOFs), and the patient can hold the handle to move in the planar space.

978-1-4799-7016-2/15/$31.00 ©2015 IEEE

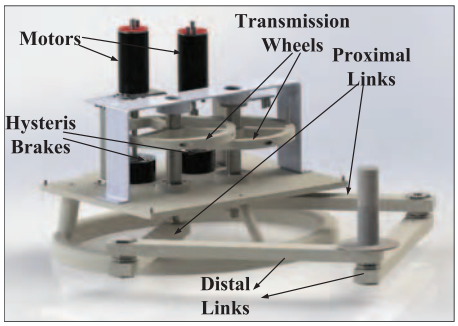

Figure 1: Rendering image of the robot mechanical design.

Parallel structures are compact and can achieve higher stiffness than serial links design [5, 6]. As the joints except the base joints are passive, the mass and inertia of the motion parts of the robot are smaller than that in serial links design.

This robot is actuated by two DC motors (RE50 by MAXON, Switzerland), which has small inertia and short response time. Besides, two hysteresis brakes are added, which are coupled with the shafts of DC motors. On one hand, DC motors based robot have stability problems in force feedback control, while the brakes are passive components and can improve the system stability [7]. On the other hand, brakes can provide more resistance together with motors in rehabilitation training, since the requirement of resistance of the robot is larger than the assistance in active training [8].

The torque outputs of motors and brakes are amplified and transmitted to the handle via a cable transmission system [9], and the transmission ratio is 20:1. Compared with the gearbox solution, cable transmission has no backlash and is backdrivable, and needs smaller-size motors than in the direct drive case [6].

Based on this design, the robot can provide a assistance above 30 N, or resistance force above 60 N at the handle within a workspace about 500 mm $\times$ 418 mm.

2.2 Control Architecture

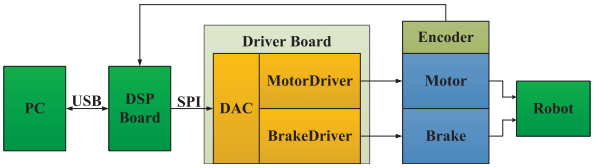

Figure 2: The architecture of the robot's control system.

As shown in Fig 2, the control system of the robot is composed of a DSP control board and a driver board, where the DSP control board can communicate with PC via USB port. On one hand, the computer sends control commands to the DSP control board, which sets the control reference to the driver board based on the commands. On the other hand, the DSP control board sends encoder values to the computer, based on which the motion information of the robot can be determined.

The driver board includes two motor driver circuits and two brake driver circuits, all of which work in the current amplification mode. Proportional-intergration (PI) current controllers are designed using operational amplifiers and discrete components, which can achieve higher bandwidth than using digital controllers and switch-type drivers.

3 KINEMATIC ANALYSIS

This section shows the robot's kinematic analysis in detail, which is the basis of robot control in following sections.

3.1 Forward Kinematics

The coordinate frame definition and schematic diagram for kinematic analysis is shown in Fig. 3, where A_1 and A_2 are the actuated joints, and B_1 and B_2 are two passive joints, and P represents the handle. In this design, two proximal links are same in length (r_1, 300 mm), and so are the distal links (r_2, 400 mm). The distance between two base joints is $2r_3$ (120 mm).

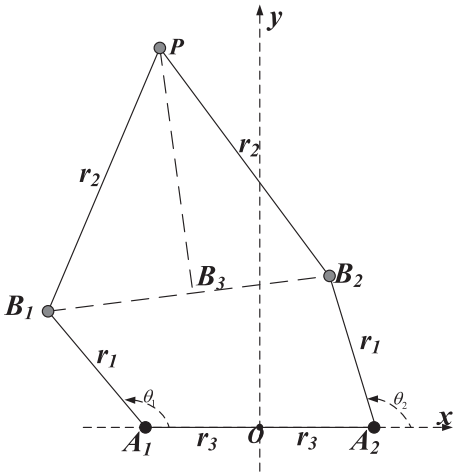

Figure 3: Coordinate frame definition and schematic diagram for kinematic analysis.

As shown in Fig. 3, the position of the handle *P* can be calculated by:

$$\mathbf{oP} = \mathbf{oB_1}+\mathbf{B_1B_3}+\mathbf{B_3P} \tag{1}$$

Depending on the known parameters of link length (r_1, r_2, r_3) and base joint angles (θ_1, θ_2), we obtain:

$$\mathbf{oB_1}=(r_1\cos\theta_1 - r_3, r_1\sin\theta_1) \tag{2}$$

$$\mathbf{oB_2} = (r_1\cos\theta_2 + r_3, r_1\sin\theta_2) \tag{3}$$

and

$$\begin{aligned}\mathbf{B_1B_2} &= \mathbf{oB_2}-\mathbf{oB_1}\\ &= (r_1\cos\theta_2 - r_1\cos\theta_1 + 2r_3,\ r_1\sin\theta_2 - r_1\sin\theta_1)\end{aligned} \tag{4}$$

As B_3 is the midpoint of B_1B_2, and two distal links have the same length, we obtain:

$$\mathbf{B_1B_3} = \frac{1}{2}\mathbf{B_1B_2} \tag{5}$$

and

$$\mathbf{B_3P} \perp \mathbf{B_1B_2} \tag{6}$$

If we define $\mathbf{B_1B_2}$ as:

$$\mathbf{B_1B_2} = (a, b) \tag{7}$$

the unit vector of $\mathbf{B_3P}$ is:

$$\left(\frac{-b}{\sqrt{a^2+b^2}}, \frac{a}{\sqrt{a^2+b^2}} \right) \tag{8}$$

As the length of $\mathbf{B_3P}$ is:

$$|\mathbf{B_3P}| = \sqrt{{r_2}^2 - \frac{a^2+b^2}{4}} \tag{9}$$

$\mathbf{B_3P}$ can be represented by:

$$\mathbf{B_3P} = \frac{(-b, a)}{\sqrt{a^2+b^2}} \times \sqrt{{r_2}^2 - \frac{a^2+b^2}{4}} \tag{10}$$

Finally, we can obtain the position of handle:

$$\begin{aligned} \mathbf{oP} &= \mathbf{oB_1} + \mathbf{B_1B_3} + \mathbf{B_3P} \\ &= \begin{pmatrix} r_1\cos\theta_1 - r_3 \\ r_1\sin\theta_1 \end{pmatrix}^T + \tfrac{1}{2}\begin{pmatrix} a \\ b \end{pmatrix}^T + \\ &\quad \frac{\sqrt{{r_2}^2 - \frac{a^2+b^2}{4}}}{\sqrt{a^2+b^2}} \begin{pmatrix} -b \\ a \end{pmatrix}^T \end{aligned} \tag{11}$$

3.2 Inverse Kinematics

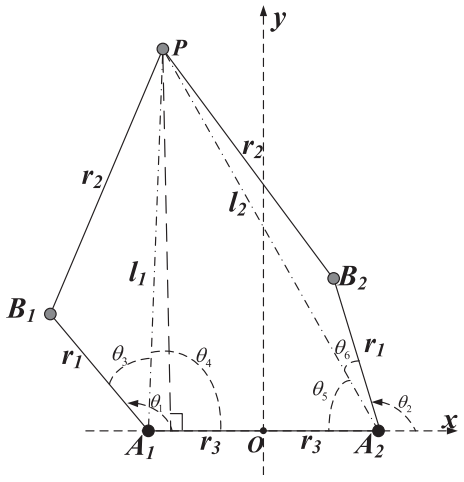

Figure 4: Coordinate frame definition and schematic diagram for inverse kinematic analysis.

As shown in Fig. 4, if the position of the handle is known as (x, y), then we obtain:

$$l_1 = \sqrt{y^2 + (x + r_3)^2} \tag{12}$$

According to the law of cosines, we obtain:

$$\theta_3 = \arccos\left(\frac{r_1^2 + l_1^2 - r_2^2}{2r_1 l_1}\right) \tag{13}$$

and

$$\theta_4 = \arccos\left(\frac{l_1^2 + (2r_3)^2 - l_2^2}{4l_1 r_3}\right) \tag{14}$$

So θ_1 can be obtained as:

$$\theta_1 = \theta_3 + \theta_4 \tag{15}$$

Similarly, we can obtain θ_2 as:

$$\theta_2 = \theta_5 + \theta_6 \tag{16}$$

where

$$\theta_5 = \arccos\left(\frac{l_2^2 + (2r_3)^2 - l_1^2}{4l_2 r_3}\right) \tag{17}$$

$$\theta_6 = \arccos\left(\frac{r_1^2 + l_2^2 - r_2^2}{2r_1 l_2}\right) \tag{18}$$

$$l_2 = \sqrt{y^2 + (x - r_3)^2} \tag{19}$$

3.3 Jacobian Derivation

As two distal links have the same length (r_2):

$$|\mathbf{B_1P}| = |\mathbf{B_2P}| = r_2 \tag{20}$$

we have:

$$\begin{cases} (x - r_1\cos\theta_1 + r_3)^2 + (y - r_1\sin\theta_1)^2 = {r_2}^2 \\ (x - r_1\cos\theta_2 - r_3)^2 + (y - r_1\sin\theta_2)^2 = {r_2}^2 \end{cases} \tag{21}$$

After we take the derivative of the above equation with respect to time, we can obtain:

$$\mathbf{A}\begin{pmatrix} \dot{\theta}_1 \\ \dot{\theta}_2 \end{pmatrix} = \mathbf{B}\begin{pmatrix} \dot{x} \\ \dot{y} \end{pmatrix} \tag{22}$$

where the two matrixes A and B are:

$$\mathbf{A} = \begin{pmatrix} y\cos\theta_1 - (x + r_3)\sin\theta_1 & 0 \\ 0 & y\cos\theta_2 + (r_3 - x)\sin\theta_2 \end{pmatrix} r_1 \tag{23}$$

and

$$\mathbf{B} = \begin{pmatrix} x + r_3 - r_1\cos\theta_1 & y - r_1\sin\theta_1 \\ x - r_3 - r_1\cos\theta_2 & y - r_1\sin\theta_2 \end{pmatrix} \tag{24}$$

Finally, the Jacobian matrix $\mathbf{J}$ can be obtained:

$$\mathbf{J} = \mathbf{B^{-1}A} \tag{25}$$

4 REALIZATION OF ACTIVE TRAINING

Active training is the main feature of existing advanced rehabilitation robots, which is proposed to make up for the deficiency of passive training.

In passive training, the robot provides all the power required for motion, and the patient's limb is led passively by the robot. Passive training is realized based on basic motion control of robot, which is easy to implement. However, passive training has proven to be less efficient for motor learning of poststroke patients in a sense that the patient

cannot feel or learn the real neuromotor outcome of their voluntary efforts [4].

On the contrary, active training is initiated and regulated by the patient, and the reaction force changes with the human voluntary effort, and the human-robot interaction is compliant rather than the stiff contact in passive training [10].

4.1 Impedance Control

Most active training are based on impedance control, which is proposed for compliant human-robot interaction. Impedance represents the dynamic relationship between motion and effort, and spring, damper, and mass are three commonly used impedances, as shown in Fig 5.

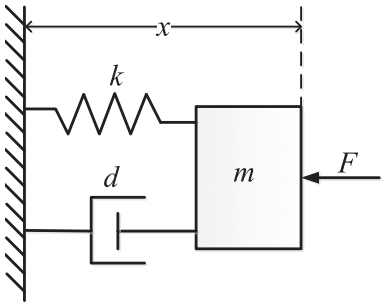

Figure 5: Impedance example of mass-damper-spring system.

The impedance relationship in Fig. 5 can be presented as:

$$F = -(k(x - x_0) + d\dot{x} + m\ddot{x}) \tag{26}$$

where x_0 is the resting point, and F is the reaction force dependent on the current position x, velocity $\dot{x}$, and acceleration $\ddot{x}$. Besides, k (spring stiffness) , d (daming) , and m (mass) are the impedance parameters [11, 12].

There are two implementation methods of impedance control. If the current motion information is available, the reaction force can be controlled based on formula (26), which is called basic impedance control method. On the contrary, if the reaction force is available, robot motion can be controlled based on formula (26), which is called admittance control or position-based impedance control [10].

4.2 Impedance Controller Implementation

As our robot is backdrivable and the motion information is available based on motor encoders, basic impedance control method is adopted in this design, which is shown in Fig 6.

As shown in Fig 6, the controller is composed of two control loops: impedance control loop and current control loop. In our design, the spring impedance part is achieved by motors, as they can produce torques in both directions; the damping impedance is realized by brakes, as they can only produce resistance according to the direction of the velocity. The mass impedance is not used in this controller, as the robot has an inherent inertia.

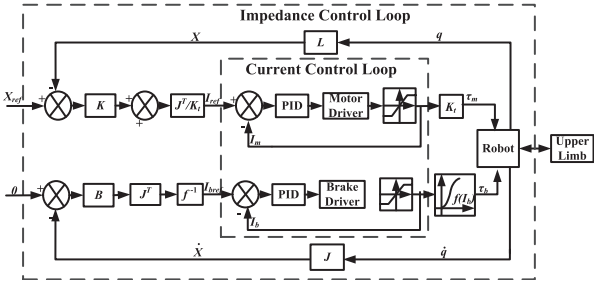

Figure 6: Control diagram of motor and brake for spring and damper impedance control, where J is the Jacobian matrix, L is the Kinematics which transmits joint space variables (q, $\dot{q}$) into Cartesian space. K_t is motor's torque constant, and f is the nonlinear torque-current relationship.

The desired reaction force at the handle can be computed according to formula (26). Then the desired reaction force is transformed into joint torques through Jacobian matrix.

$$\tau = J^T F \tag{27}$$

As the torque of the DC motor is proportional to its current, the current reference is computed as desired motor torques dived by torque constant K_t. On the contrary, the relationship between the brake torque and current is nonlinear, and the relationship f is obtained by experiment and curve fitting using a torque sensor.

The kinematic computation and impedance controller is realized on PC by C++ programming, and the desired torques are transmitted to the robot, and the control loop is updated every 1 ms.

4.3 Active Training and Virtual Reality

In order to perform active training and provide direction to the patient, some training games were designed based on virtual reality techniques. Virtual reality environment can be found in most advanced rehabilitation robots, and it works as a visual feedback to the patient.

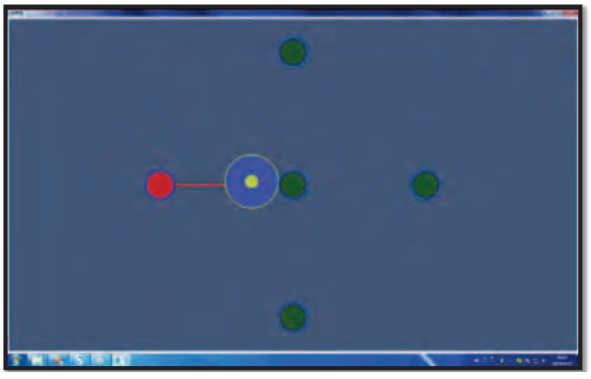

Figure 7: Reaching game user interface.

In this experiment, a simple game was designed to help improve the patient's reaching ability. As shown in Fig. 7, the patient was directed to move his hand from one point to the target. The interaction force was controlled by the

impedance controller, and a virtual spring was connected between them, which means the closer the patient was to the target, the more resistance was posed by the robot.

Meanwhile, the patient was asked to move along a straight line between the starting point and target point, which was the most efficient path as a normal human did. For this end, two stiff virtual walls were built at both sides of the straight path. If the patient deviated from the straight path, he/she would be bounced back by the virtual walls.

4.4 Results of System Control

In order to evaluate the performance of the proposed control method, a 3-axis force sensor was installed at the handle, which can detect the interaction force between the robot and patient.

As the robot moves in a planar workspace, only X and Y outputs of the force sensor were used (shown in Fig. 8), where the Y axis was installed along the right distal link.

In order to compare the target force and actual force, the force sensor outputs should be transformed into the base coordinate system.

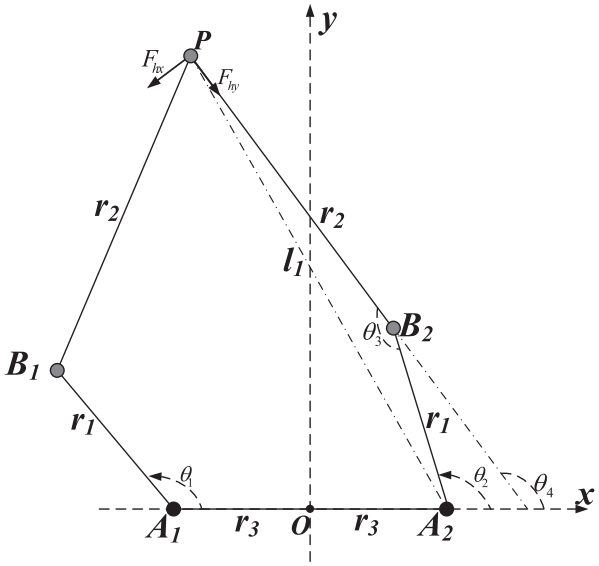

Figure 8: Coordinate frame definition and schematic diagram for reaction force computation, where F_{hx} and F_{hy} represent the force sensor outputs of X channel and Y channel respectively.

As shown in Fig. 8, the reaction force can be represented in the base coordinate system as:

$$\mathbf{F_h^0} = \mathbf{R_h^0}[F_{hx}, F_{hy}]^T \tag{28}$$

where $\mathbf{R_h^0}$ is the transmission matrix from the handle coordinate system to the base coordinate system, and $\mathbf{F_h^0}$ is the force vector represented in the base coordinate, and $[F_{hx}, F_{hy}]^T$ is the force vector represented in the handle coordinate.

The transmission matrix $\mathbf{R_h^0}$ can be obtained as:

$$\mathbf{R_h^0} = \begin{bmatrix} -\sin\theta_4 & -cos\theta_4 \\ \cos\theta_4 & -\sin\theta_4 \end{bmatrix} \tag{29}$$

As $\theta_4 = \theta_2 + \pi - \theta_3$, formula (28) can be transformed into:

$$\mathbf{F_h^0} = \begin{bmatrix} -F_{hy} & -F_{hx} \\ F_{hx} & -F_{hy} \end{bmatrix} \begin{bmatrix} -\cos\theta_2 & -\sin\theta_2 \\ -\sin\theta_2 & \cos\theta_2 \end{bmatrix} \begin{bmatrix} \cos\theta_3 \\ \sin\theta_3 \end{bmatrix} \tag{30}$$

According to the law of cosines, we obtain:

$$\begin{cases} \cos\theta_3 = \frac{r_1^2 + r_2^2 - l_1^2}{2r_1 r_2} \\ \sin\theta_3 = \sqrt{1 - (\cos\theta_3)^2} \end{cases} \tag{31}$$

where $l_1^2 = |\mathbf{PA_2}|^2 = (x - r_3)^2 + y^2$.

The comparison result of the target force and actual reaction force is shown in Fig. 9 , where the data was recorded when the subject performed the target reaching game mentioned above.

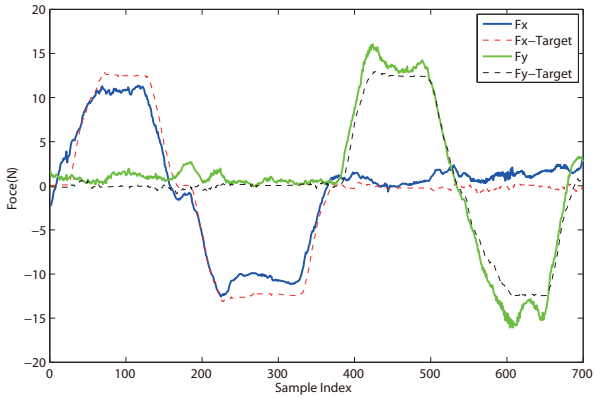

Figure 9: Comparison of the target and actual reaction force in two directions, where the solid lines represent the actual reaction force, and the dotted lines represent the target force.

As shown in Fig. 9, the actual reaction force can follow the the target force well, and the average error between the controlled and target reaction force is 1.41 ± 0.79 N in the X axis, and 1.22 ± 0.91 N in the Y axis.

REFERENCES

[1] V. Klamroth-Marganska, J. Blanco, K. Campen, A. Curt, V. Dietz, T. Ettlin, M. Felder, B. Fellinghauer, M. Guidali, A. Kollmar, A. Luft, T. Nef, C. Schuster-Amft, W. Stahel, and R. Riener, "Three-dimensional, task-specific robot therapy of the arm after stroke: a multicentre, parallel-group randomised trial," *The Lancet Neurology*, vol. 13, no. 2, pp. 159–166, 2014.

[2] A. C. Lo, P. D. Guarino, L. G. Richards, J. K. Haselkorn, G. F. Wittenberg, D. G. Federman, R. J. Ringer, T. H. Wagner, H. I. Krebs, B. T. Volpe, C. T. Bever, D. M. Bravata, P. W. Duncan, B. H. Corn, A. D. Maffucci, S. E. Nadeau, S. S. Conroy, J. M. Powell, G. D. Huang, and P. Peduzzi, "Robot-assisted therapy for long-term upper-limb impairment after stroke," *New England Journal of Medicine*, vol. 362, no. 19, pp. 1772–1783, 2010.

[3] R. Riener, T. Nef, and G. Colombo, "Robot-aided neurorehabilitation of the upper extremities," *Medical and Biological Engineering and Computing*, vol. 43, no. 1, pp. 2–10, 2005.

[4] N. Hogan, H. I. Krebs, B. Rohrer, J. J. Palazzolo, L. Dipietro, S. E. Fasoli, J. Stein, R. Hughes, W. R. Frontera, D. Lynch, and B. T. Volpe, "Motions or muscles? some behavioral factors underlying robotic assistance of motor recovery," *Journal of rehabilitation research and development*, vol. 43, no. 5, pp. 605–618, 2006.

[5] H. V. Minh and N. Uhn-Joo, "Tele-operation of a 6-dof serial robot using a new 6-dof haptic interface," in *Proceedings of IEEE International Symposium on Haptic Audio-Visual Environments and Games (HAVE)*, 2010, pp. 1–6.

[6] G. Campion, W. Qi, and V. Hayward, "The pantograph mk-ii: a haptic instrument," in *Proceedings of IEEE/RSJ International Conference on Intelligent Robots and Systems (IROS)*, 2005, pp. 193–198.

[7] J. J. Gil, A. Avello, A. Rubio, and J. Florez, "Stability analysis of a 1 dof haptic interface using the routh-hurwitz criterion," *IEEE Transactions on Control Systems Technology*, vol. 12, no. 4, pp. 583–588, 2004.

[8] D. Chapuis, R. B. de Grave, O. Lambercy, and R. Gassert, "Reflex, a haptic wrist interface for motor learning and rehabilitation," in *Proceedings of IEEE Haptics Symposium*, 2010, pp. 417–424.

[9] T. Nef and R. Riener, "Armin - design of a novel arm rehabilitation robot," in *Proceedings of International Conference on Rehabilitation Robotics (ICORR)*, 2005, pp. 57–60.

[10] H. Jin, H. Zengguang, Z. Feng, C. Yixiong, and L. Pengfeng, "Training strategies for a lower limb rehabilitation robot based on impedance control," in *Proceedings of Annual International Conference of the IEEE Engineering in Medicine and Biology Society (EMBC)*, 2012, pp. 6032–6035.

[11] N. Hogan, "Impedance control: An approach to manipulation," in *Proceedings of American Control Conference*, 1984, pp. 304–313.

[12] L. Marchal-Crespo and D. Reinkensmeyer, "Review of control strategies for robotic movement training after neurologic injury," *Journal of NeuroEngineering and Rehabilitation*, vol. 6, no. 1, p. 20, 2009.